Analytica Chimica Acta 1171 (2021) 338665

Contents lists available at ScienceDirect

Analytica Chimica Acta

journal homepage: www.elsevier.com/locate/aca

In-tube solid phase microextraction coupled to miniaturized liquid chromatography for both, noble metal nanoparticle assessment and sensitive plasmonic assay development

L. Sanjuan-Navarro , S. Cortés-Bautista , Y. Moliner-Martínez , P. Campíns-Falcó *

MINTOTA Research Group, Departament de Química Analítica, Facultat de Química, Universitat de Valencia, 46100, Burjassot, Spain

HIGHLIGHTS

- In tube-SPME and Miniaturized LC as a new tool for plasmonic assays.
- Assessment of noble NPs from the ratio of two chromatographic peaks in 10 min.
- Improved sensitivity and selectivity for spermine and H^+ - induced assays.
- Urine samples for healthy volunteers and cancer patients were tested.

GRAPHICAL ABSTRACT

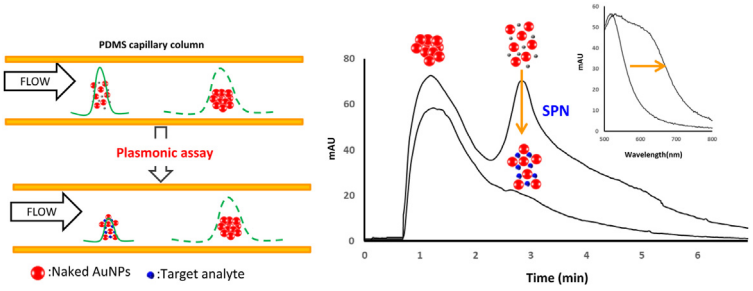

ARTICLE INFO

Article history:
Received 6 January 2021
Received in revised form
16 May 2021
Accepted 17 May 2021
Available online 21 May 2021

Keywords:
Plasmonic assay
Miniaturized liquid chromatography
In-tube SPME
Acids
Spermine
Urine sample
Noble nanoparticle assessment

ABSTRACT

Colorimetric localized surface plasmon resonance (LSPR) as analytical response is applied for a wide number of chemical sensors and biosensors. However, the dependence of different factors, such as size distribution of nanoparticles (NPs), shape, dielectric environment, inter-particle distance and matrix, among others, can provide non-reliable results by UV–vis spectrometry in complex matrices if NP assessment is not carried out, particularly at low levels of analyte concentrations. Miniaturized liquid chromatography, capillary (CapLC) and nano (NanoLC), coupled on line with in-tube solid phase microextraction (IT-SPME) is proposed for the first time for both, controlling suitability of used noble metal NP dispersions and developing plasmonic assays. Several capped noble NPs and target analytes were tested from variations in the chromatographic profiles obtained by using diode array detection. The IT-SPME step, which influenced the chromatographic fingerprint provided by noble NP dispersions, was studied by asymmetrical flow field flow fractionation (AF4) too. We monitored NP aggregation induced by interaction with several analytes like acids and spermine (SPN). Assessment of NPs was achieved in less than 10 min and it permitted to develop suitable plasmonic tests. Here, it was also demonstrated that these assays can be followed by IT-SPME-miniaturized LC-DAD and more sensitivity and selectivity than those provided by UV–Vis spectrometry were achieved. Analysing urine samples to determine SPN as a cancer biomarker as a proof of concept is presented.

1. Introduction

Noble metal nanoparticles (NPs) like AuNPs and AgNPs, are especially suitable for sensing applications since they possess high

* Corresponding author.
E-mail address: pilar.campins@uv.es (P. Campíns-Falcó).

https://doi.org/10.1016/j.aca.2021.338665
0003-2670/

extinction coefficients in the visible region due to the strong localized surface plasmon resonance (LSPR) [1,2]. Among the different LSPR sensing strategies, the colorimetric assays that benefit from the aggregation as readout are widely used [3–5]. This strategy has been proposed in different approaches for compounds of chemical or biological interest, such as spermine [5–8], dopamine [9], creatinine [10], DNA [11] or enzymes [12]. The application of these strategies has been recently reviewed by Kailasa et al. [13] showing the benefits and limitations of these assays.

Despite the advantages, one of the main limitations in practical applications is the lack of reproducibility of NP dispersions induced by solvents, pH, atmosphere, temperature or other compounds present in the matrix [14]. Particle size and stability analysis are also key elements for their practical applications since the NPs properties depend on these parameters. In a previous paper, we used asymmetrical flow field flow fractionation (AF4) coupled to UV–Vis and dynamic light scattering (DLS) detectors in series, for stability studies of citrate-capped AuNPs and AgNPs aqueous dispersions [15].

Similar to the plasmon resonance band, the aggregation profile and thus, the optical readout by UV–Vis spectroscopy depends on the size distribution, shape and dielectric environment of the starting NPs, and thereof monitoring of plasmonic colorimetric assays, which can provide non-reliable results in complex matrices if NP assessment is not carried out. A potential strategy to obtain more reliable results can be the isolation of the responses as a function of the main factor affecting the analytical signal. Miniaturized LC- DAD responded linearly to NP concentration as we showed in Refs. [16,17] and also to NP size, a property that can be mathematically related to concentration. The flow in miniaturized LC and the diffusion through the pores (on the same order of magnitude as the diameters of the studied NPs), condition the particle interactions through the system in a dynamic process. Although UV–Vis spectrophotometry is not suitable for the estimation of NP concentration, DAD detection under these above mentioned chromatographic conditions allows one to do so [16,17]. Besides, we studied the combination of in-tube solid phase microextraction (IT-SPME) [18] with capillary liquid chromatography (CapLC) with DAD detection for characterizing dispersions of metallic nanoparticles [16,17]. In this approach, the chromatographic response of noble nanoparticle dispersions provided two chromatographic peaks, which responded to the existence of different NPs distributions in the bulk dispersion: non-polarized NPs which interact with the IT-SPME extractive phase by a hydrophobic effect, and water polarized AgNPs governed by a size exclusion mechanism in the analytical column. The peak ratio for a given dispersion allows the estimation of the average diameter of noble NPs and permits to study stability and functionality related properties. The area or height of the chromatographic peaks are related with the NP concentration. The IT-SPME step, which influences the chromatogram fingerprint provided by noble NP dispersions, was studied here by AF4 for the first time.

In previous studies, the potential of mainly IT-SPME-CapLC was reported for characterizing noble NP dispersions. The objective of the present work was to evaluate IT-SPME-CapLC and NanoLC-DAD for both, to assess NPs and to monitor LSPR responses in plasmonic assays. For this aim, spermine [5] and [H^+]-induced colorimetric assays [15] were selected as targets using several capped NPs. First, the chromatographic profile of the NP dispersions was studied in order to stablish the two populations of the NPs in the bulk dispersion. Mixtures of AuNPs and AgNPs were also investigated. Here, we demonstrated that the chromatographic profile of the two mentioned populations determines the successful application of the NPs for LSPR sensing strategies based on their aggregation, since they are related with NPs properties and their chemical environment. Besides, we demonstrated that these techniques can be also used for following plasmonic assays. Spermine as a cancer biomarker in urine is studied as proof of concept.

2. Experimental section

2.1. Reagents

Gold (III) tetrachloroauric acid trihydrate 99.99% ($HAuCl_4 \cdot 3H_2O$), 50% H_2O_2, manganese dioxide (MnO_2) and Chelex 100 from Sigma-Aldrich (USA) were used for AuNPs synthesis [16]. Cap-LC mobile phase was prepared with sodium dodecyl sulfate (SDS, >99%, Panreac, Spain), ammonium acetate ($AcNH_4$, 98%, Panreac) and sodium thiosulfate ($Na_2S_2O_3$, Scharlab, Spain). Gold nanoparticles (20 nm, 40 nm core) some stabilized in citrate buffer and others in phosphate-buffered saline (PBS) and silver nanoparticles (20 nm, 40 nm core) stabilized in citrate buffer (Sigma-Aldrich) were used for acid aggregation assays. Spermine (>99%, Sigma-Aldrich), acetic acid (HAc, Scharlab), *o*-phosphoric acid (H_3PO_4, Sigma-Aldrich), hydrochloric acid (HCl, Scharlab), acetonitrile (CH_3CN, VWR Chemicals, USA), hydrogen carbonate ($NaHCO_3$, Panreac) and methanol (MeOH, VWR Chemicals) were used for additional tests and assays. Water was purified through a Sybron Barnstead NANOpure II system.

2.2. Instrumentation

UV–Visible spectra were registered with a Varian Cary 60 Fiber Optic UV–Vis spectrophotometer. The analytical signal was recorded between 200 and 800 nm.

Chromatographic studies were carried out using an Agilent Technologies high performance liquid chromatographic system equipped with a LC capillary binary gradient pump (Agilent 1200 Series) coupled to a diode array detector (DAD). A Jupiter C18 column (5 μm, 300 Å, 0.5 mm i.d. x 5 cm) was used as analytical column. IT-SPME was performed by using a capillary column of polydimethylsiloxane (PDMS) with 35% of polydiphenylsiloxane (TRB-35) (Teknokroma, Spain).

For some acid aggregation studies, an Agilent Technologies high performance liquid chromatographic system equipped with a LC nano binary gradient pump (Agilent 1200 Series) coupled DAD was employed. A ZORBAX 300SB-C18 (3.5 μm, 300 Å, 0.075 × 50 mm) was used as analytical column. IT-SPME was performed by using a synthesized capillary column of tetraethyl orthosilicate (TEOS)-tetramethyl orthosilicate (MTEOS)- silica nanoparticles ($NPSiO_2$), which was synthetized by using the procedure proposed in Ref. [19].

AF4 system (AF200 Postnova Analytics, Germany) was used. The channel used was 29 cm long with spacer of 350 μm and a regenerated cellulose membrane with a 10 kDa cutoff. The flows were provided by two separate pumps and the cross-flow was realized by a separate piston pump which is continuously adjustable. The eluent was ultrapure water with 0.02% NaN_3 and the flow kept at 0.5 mL min^{-1}. Optimal signal was achieved using a linear gradient cross-flow (10 mL) for the first 30 s and then 0 mL min^{-1} for the last 10 s. The output of the channel was connected to an on-line UV–Vis spectrometer set at 410 nm wavelength for detection of AgNPs. The injection volume was 20 μL for all analyses.

2.3. Synthesis of naked gold nanoparticles

Synthesis of AuNPs was performed following the procedure described in Ref. [5]. An aqueous solution of 0.5–1.2 mM H_2O_2 and 0.5 mM $HAuCl_4$ in Millipore water (treated overnight with Chelex to eliminate metal traces in water) was irradiated with a 532 nm laser (10 Hz, 16–19 mL) until the Au^{3+} band (ca. 300 nm) disappeared

and that of H_2O_2 (240 nm) decreased to approach the absorbance of the plasmon band at 520–525 nm. After dilution of the mixture with water (2:1 H_2O:AuNP solution), the excess of H_2O_2 was removed by using UVA-lamp irradiation for 20 min [20]. UV–Vis spectra were registered with a Varian Cary 60 Fiber Optic UV–Vis spectrophotometer. The analytical signal was recorded between 200 and 800 nm.

2.4. Spectrophotometric measurements

In this work, the LSPR response was obtained following the procedure: different volumes of standard or sample were mixed with 300 μL of ultrapure H_20 and 300 μL of NPs. The spectrophotometric studies were carried out by registering the spectra between 300 and 800 nm. Kinetic study was performed by measuring the spectra during 10 min in intervals of 20 s.

To carry out the acid aggregation assay, nanoparticle dispersions were prepared mixing different volumes of commercial NPs with ultrapure water and then adding the adequate amount of HAc solutions. Citrate and phosphate capped gold nanoparticles diluted at 25% (v/v) containing HAc 10% (v/v) were obtained by mixing: 250 μL of AuNPs, 300 μL of water, then 300 μL of HAc 20% (v/v) was added reaching a final volume of 1 mL. Citrate capped silver nanoparticles diluted at 50% (v/v) in HAc 0.2% (v/v) were prepared by mixing: 500 μL of AgNPs with 300 μL of water, then 200 μL of HAc 1% (v/v) was added to a final volume of 1 mL. Silver and gold citrate capped nanoparticles mixtures diluted at 25% (v/v) in HAc 0.7% (v/v) were prepared by mixing: 150 μL of AgNPs and 150 μL of AuNPs with 220 μL of water, then 80 μL of HAc 1% (v/v) was added to a final volume of 600 μL.

HAc 20% and 1% (v/v) solutions were prepared taking 20 and 1 mL, respectively, of acetic acid glacial and making up to 100 mL with water.

2.5. Chromatographic conditions

A mixture of 10 mM ammonium acetate, 10 mM SDS and 1 mM sodium thiosulfate prepared in water previously filtered with nylon filters (0.45 μm) was used [16]. The mobile phase was ultrasonicated for 45 min previous to its use.

Working flow rate was 12 μL min^{-1} for CapLC and 0.5 μL·min^{-1} for NanoLC. Then, 20 μL or 10 μL of standards or samples were processed into CapLC or NanoLC, respectively. IT-SPME capillaries as injection loops of 20 cm and 15 cm lengths were employed for CapLC and NanoLC, respectively (see Fig. 1). Typically, the sample was passed through the IT-SPME capillary for its clean-up, extraction and preconcentration of analytes. Then, the valve was rotated to injection position and the analytes were transferred to the analytical column for their separation and detection. DAD detector registered the spectra between 300 and 800 nm. The IT-SPME CapLC and NanoLC set up are shown in Fig. 1. After each session, the chromatographic system was conditioned with mobile phase (15 min), water (15 min) and EtOH (30 min).

2.6. Off-line IT-SPME and AF4

Off-line IT-SPME and AF4-UV-Vis-DLS analysis were carried out using a six-port injection valve and IT-SPME capillary column of polydimethylsiloxane (PDMS) with 35% of polydiphenylsiloxane (24.3 cm length, 0.32 mm i.d and 3 μm thinkness; 20 μL). The extraction phase consisted of a mixture of 10 mM ammonium acetate, 10 mM SDS and 1 mM sodium thiosulfate prepared in water previously filtered with nylon filters (0.45 μm) as the mobile phase in miniaturized chromatography [16]. The extraction phase was ultrasonicated for 45 min previous to its use.

The procedure performed had the next steps: first, 20 μL of AgNPs bulk dispersion (20 nm core) were injected in IT-SPME capillary column (20 μL), after 20 μL of extraction phase were injected and the extracted solution was collected. Then, 140 μL of ultrapure water were added to the solution (1:8 dilution) and 20 μL was injected in the AF4-UV-Vis-DLS system, obtaining the corresponding signal named "First Extraction". The second step, consisted in injecting another 20 μL of extraction phase in the IT-SPME capillary column, the extract solution was recollected and it was diluted with 140 μL of ultrapure water, and after 20 μL were injected in the AF4 system. This step was repeated 4 times, obtaining successive extractions (since first to sixth extractions). The results were compared with a direct injection of AgNPs diluted 1/8 with ultrapure water by using the AF4 stainless loop (20 μL).

2.7. Monitoring of plasmonic assays

In this work several plasmonic assays were carried out: spermine plasmonic assay by using naked AuNPs and acid induced aggregations of naked AuNPs; citrate and phosphate capped AuNPs, citrate capped AgNPs and mixtures of citrate capped AuNPs and

System/IT-SPME capillary	A			B			C			D			V total (μL)
	L cm	i.d. μm	V μL	L cm	i.d. μm	V μL	L cm	i.d. μm	V μL	L cm	i.d. μm	V μL	
CapLC/TRB-35	20	320	16.1	12	50	0.24	5	500	9.81	20	25	0.10	26.25
NanoLC/TEOS-MTEOS-SiO_2	15	75	0.66	10	25	0.05	5	75	0.22	20	25	0.10	1.03

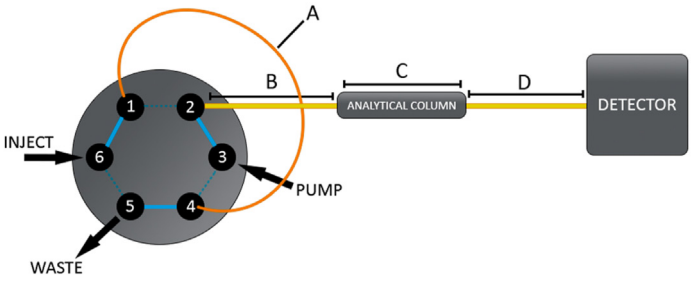

Fig. 1. IT-SPME-CapLC and NanoLC –DAD devices and their dimensions.

AgNPs and acid induced aggregations. In the former, SPN standards and urine samples were used to evaluate the IT-SPME CapLC profile of colorimetric LSPR assay proposed in Ref. [5]. Briefly, SPE using C18 silica cartridges (100 mg, Phenomenex, EEUU) were conditioned with methanol (1 mL) and hydrogen carbonate solution (1 mL, 0.5 M) at pH 12. Then, 1 mL of standards or urine was passed through the cartridge. After, a clean-up step with hydrogen carbonate solution (2 mL), acetonitrile (1 mL) and ultrapure water (2 mL) was carried out. The elution was carried out by using HAc 5% in two fractions of 0.25 mL each. Finally, aliquots of the elution with AuNPs solution (300 μL AuNPs + 300 μL ultrapure water) were injected in the chromatographic system or analyzed by using spectroscopy measurements. SPN was assayed up to 600 μg L^{-1} (see Figure S2 of SI).

Studies of [H^+]-induced aggregation by IT-SPME CapLC were performed using different additions of acid taking the adequate amount of the standard (HAc 5%, HCl 0.2% and H_3PO_4 0.2%) to 300 μL of ultrapure water and 300 μL AuNPs. Naked AuNPs and commercial NPs were assayed.

In order to carry out acid aggregation assay by IT-SPME NanoLC, commercial nanoparticle dispersions were prepared mixing different volumes of commercial NPs with water and then adding the adequate amount of HAc solutions. Citrate and phosphate capped gold nanoparticles diluted at 25% (v/v) in HAc 10% (v/v) were obtained from 250 μL of bulk AuNPs, 250 μL of water and 500 μL of HAc 20% (v/v) reaching a final volume of 1 mL. Citrate capped silver nanoparticles diluted at 50% (v/v) in HAc 0.2% (v/v) were prepared mixing 500 μL of AgNPs with 300 μL of water, then 200 μL of HAc 1% (v/v) was added to a final volume of 1 mL. Citrate capped silver and gold nanoparticles mixture diluted at 25% (v/v) in HAc 0.7% (v/v) were prepared mixing 150 μL of AgNPs and 150 μL of AuNPs with 280 μL of water, then 20 μL of HAc 20% (v/v) was added to a final volume of 600 μL.

3. Results and discussion

3.1. Nanoparticle assessment

The IT-SPME step, which influenced the chromatogram fingerprint, was studied by AF4. Fig. 2 shows two groups in the fractogram in function of the processed LC-mobile phase volume for 1:8 water diluted AgNPs (20 nm core and citrate capping). This figure also shows the chromatogram obtained by coupling on-line IT-SPME and CapLC with DAD detection. The non polarized group of NPs (second chromatographic peak) required higher volumes of mobile phase to leave the IT-SPME capillary and presented smaller hydrodynamic diameter that the water polarized NPs (first chromatographic peak). These results are in accordance with the separation mechanisms stablished in Ref. [16] for IT-SPME–CapLC-DAD (see Fig. 2). Only one population is observed if direct injection with a stainless loop is carried out, similar to the signal obtained in Ref. [16] by CapLC-DAD without coupling IT-SPME. Polarized population elutes first from the IT-SPME capillary because their interaction is weak with the film phase, meanwhile non-polarized population interacts with the IT-SPME phase eluting after as AF4 demonstrates.

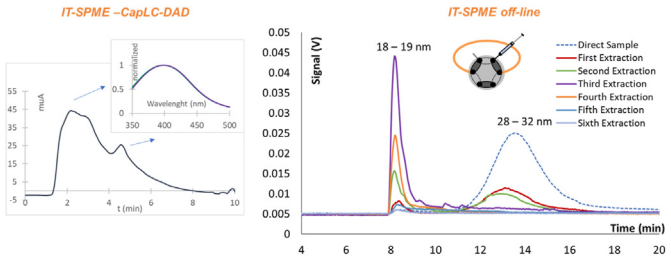

Fig. 2. On-line IT-SPME-CapLC-DAD (inset: normalized spectra obtained at the maximum of the two chromatographic peaks) and off-line IT-SPME and AF4 results for 1:8 ultrapure water diluted dispersion of AgNPs (20 nm core; citrate capping). For more explanation see text.

Fig. 3a shows the chromatographic profiles of commercial citrate capped NPs of different size, which were dependent of size and metal. The miniaturized LC systems improved sensitivity and resolution, less sample dilution and diffusion effects are achieved in reference to conventional LC and IT-SPME coupling permits to detect differences in the distribution of polarized and non-polarized noble NPs in the bulk dispersion. The peak at lower retention time (t_r), was characterized by a minimal interaction with the IT-SPME extractive phase; and thereof the separation mechanism was attributed to size exclusion interactions in the analytical column [16]. The identification of a second peak at higher t_r, demonstrated the presence of a stronger interaction between the noble NPs distribution and the IT-SPME extractive phase. Taking into account the apolar nature of the coating, this separation can be explained by means of hydrophobic effect [16]. Based on these results, the differences in the distribution of polarized and non-polarized noble NPs in the bulk dispersion can be used to differentiate them.

Several target analytes of different nature were chosen to study the aggregation profiles of the several assayed NPs by UV–vis spectrometry. Fig. 3b–e shows the aggregation profiles obtained as a function of time for some commercial NPs by adding acetic acid. For the same capping and size, AgNPs provided more sensitivity than AuNPs for acetic acid aggregation (see Fig. 3b and c). When the two type of noble NPs were employed together the responses were additive as it can be seen in Fig. 3d. Spermine was also assayed, but no aggregation was obtained at levels assayed for these kind of NPs. The extension of aggregation depended on the capping of AuNPs for the same size as it can be seen in Fig. 3, c and e.

The sensitivity of AuNPs as sensors can strongly depend on the accessibility of the analyte to their surface; the more naked they are, the more sensitive they will be [5]. Fig. 4 shows the profiles obtained for six batches of synthetized naked AuNPs. The profiles for the different batches of AuNPs (dilution 1:1 of the bulk dispersion) showed differences in the distribution of polarized and non-polarized AuNPs in bulk dispersions. Attending to these differences, the naked AuNPs were classified into two groups: Group I: similar polarized and non-polarized distribution in the bulk dispersion [AuNPs(I)] (Fig. 4a), and Group II: predominant polarized NPs distribution in the bulk dispersion [AuNPs(II)] (Fig. 4b) as for commercial AuNPs (see Fig. 3). It should be noted that the hydrodynamic diameters were 17.46 nm and 21.20 nm for AuNPs(I) and AuNPs(II) bulk dispersion estimated by static DLS measurements, respectively, showing low differences in the NPs sizes and similar to commercial AuNPs 20 nm. Fig. 4 shows that UV–Vis spectroscopy provides similar spectra for both, AuNPs(I) and AuNPs(II) and then, any discrimination can be done by this technique.

The aggregation profiles obtained by UV–Vis spectroscopy for each group of naked AuNPs as a function of successive additions of acetic acid and SPN are shown in Figure S1 and Figure S2 of the supporting information (SI), respectively. It should be noted that concentration levels for HAc was up to mM to observe aggregation effects by it for naked AuNPs (I). As can be seen, in Figure S1a, aggregation was not observed at concentration level up to 0.8 mM of HAc, which meant they remained stable upon the addition of HAc. However, at higher concentration level, we observed aggregation as a linear function of the concentration level of HAc, resulting in an

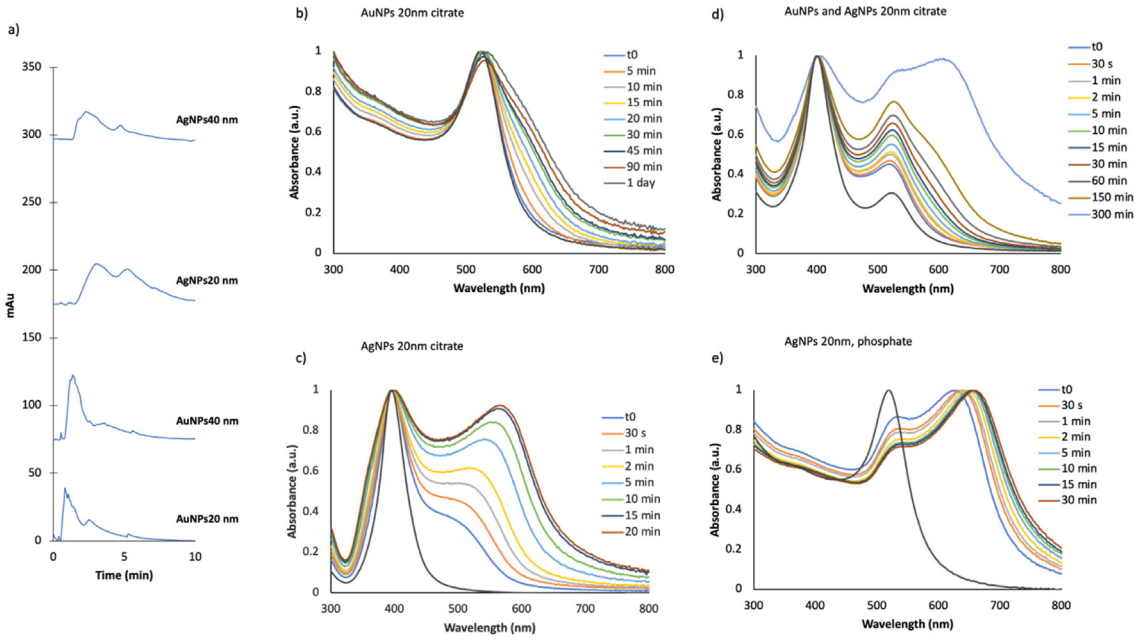

Fig. 3. Chromatographic profile of commercial noble citrate capped NPs (a) and aggregation profiles due to acetic acid as a function of time of: citrate capped AuNPs 20 nm diluted 1:4 in HAc 10% (v/v) (b) and diluted 1:2 in HAc 0.2% (v/v) (c), a mixture of citrated capped AuNPs and AgNPs 20 nm diluted 1:4 in HAc 0.7% (v/v) (d) and phosphate capped AgNPs 20 nm diluted 1:4 in HAc 0.2% (v/v) (e) obtained by UV–Vis spectroscopic measurements. (For more details see Experimental section).

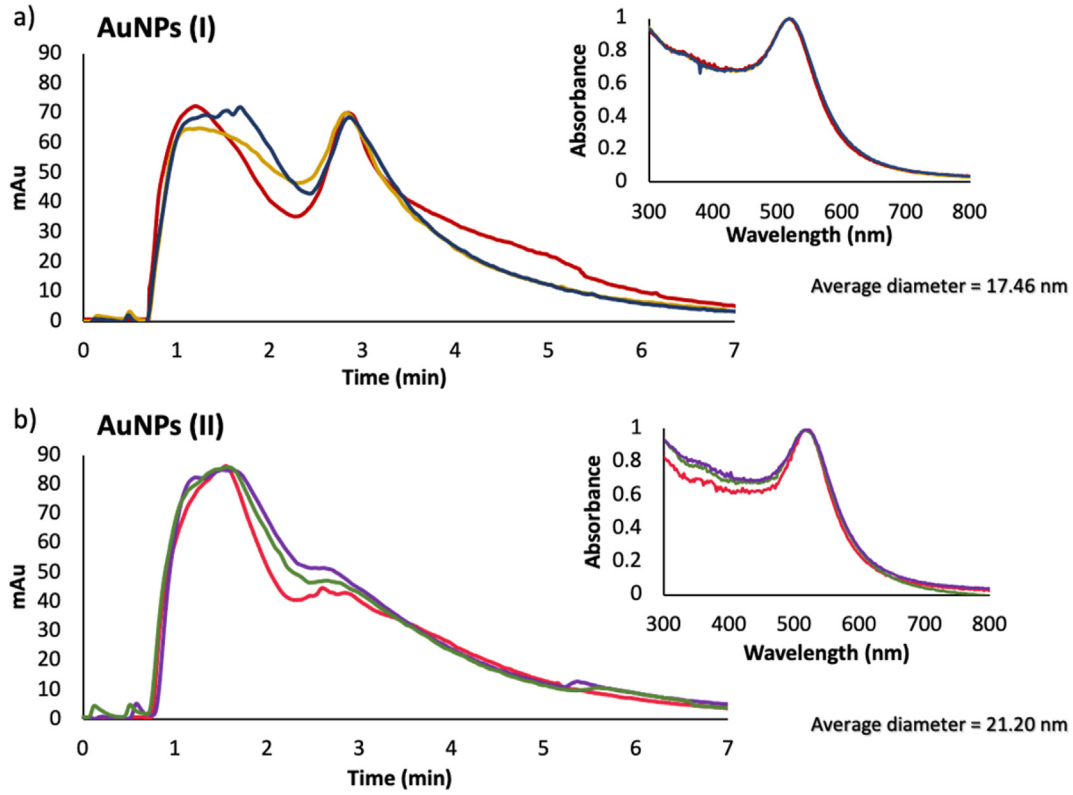

Fig. 4. (a) Chromatographic profiles obtained for three batches of naked AuNP corresponding to AuNPs(I). (b) Chromatographic profiles obtained for three batches of naked AuNP corresponding to AuNPs(II). Insets: UV–Vis Spectra for both types of naked AuNPs.

interval up to 2 mM (Figure S1c). AuNPs(II) group aggregated with a different profile than AuNPs(I) group. As can be seen, in Figure S1(b and c), these NPs were aggregated at concentration lower than 0.4 mM of HAc and the saturation was reached up 1.2 mM. Therefore, in terms of plasmonic assays, AuNPs(I) and AuNPs(II) could be used to monitor interaction with $[H^+]$, depending on their concentration levels.

The behavior of naked AuNPs(I) and AuNPs(II) showed

significant differences for SPN, these can be seen by comparing Figure S2, a and b. Working concentration interval for SPN was up to 40 μg L^{-1} for AuNPs(II), meanwhile for AuNPs(I) was up to 250 μg L^{-1}, see Figure S2 (c and d), respectively. Indeed, signal saturation was reached at different concentration levels depending on the AuNPs used. These results can be correlated with the different chromatographic profiles obtained for AuNPs(I) and AuNPs(II). The AuNPs with predominant polarized distribution provided the lower aggregation concentration interval, however, AuNPs showing both effects (see Fig. 4) (polarized and non-polarized) provided extended aggregation concentration intervals, which corresponded to AuNPs(I). AuNPs(I), in presence of HAc at concentration up to 0.8 mM can be suitable to monitor other analytes (see Figure S1c), since these concentrations did not aggregated NPs.

Hence, these results indicated that AuNPs(I) were suitable to monitor SPN and [H^+], however AuNPs(II), would not be suitable to monitor SPN, and only interaction with [H^+] can be studied as commercial citrate capped AuNPs 20 nm, both of them with similar chromatographic profiles. IT-SPME coupled to miniaturized LC is a powerful tool for stablishing the suitability of a given batch to carry out a given plasmonic assay as it is demonstrated here employing less than 10 min.

3.2. Monitoring plasmonic assays by IT-SPME-miniaturized LC-DAD

The next step was to evaluate the use of the IT-SPME-CapLC-DAD and IT-SPME-NanoLC-DAD for developing plasmonic assays. Fig. 5 depicts the variation of the chromatographic profiles of naked AuNPs(I) as a function of the addition of SPN and acetic acid. The addition of SPN or acetic acid to a dispersion of naked AuNPs(I) gave rise to the aggregation of AuNPs, that was observed by means of the color change from red to blue purple (Fig. 5a). Fig. 5b shows a scheme of the separation achieved in the IT-SPME capillary in accordance with the two populations, polarized and non-polarized provided for each batch dispersion. These assays are based on the absence of a competitive organic capping on the naked gold nanoparticles and together with the high affinity of the amine groups for the nanoparticle surface for spermine [5]. As can be seen in Fig. 5c and d, the successive analyte additions resulted in changes in area of the two peaks and in the ratio between the two peaks for spermine additions. The variation of the spectra profile for chromatographic peak at 3 min showed that the decrease in the peak area was directly related with the variation of the LSPR signal due to aggregation of AuNPs since it was observed the band shift depending on the SPN concentration in the sample (see Fig. 5c, insets). As can be seen, the first chromatographic peak did not response to the SPN concentration. At low SPN concentration, aggregation was only observed in the peak corresponding to non-polarized AuNPs. At concentrations higher than 66 μg L^{-1}, the first peak also decreases.

Sensitivity of the assay by IT-SPME-CapLC-DAD was higher than that achieved by spectrophotometric measurements (see Figure S2, a and c, and Fig. 5c). Fig. 5c showed a progressive aggregation as a function of the SPN concentration (41, 66 and 82 μg L^{-1}), which gave rise to a good discrimination of SPN concentrations (Fig. 5c

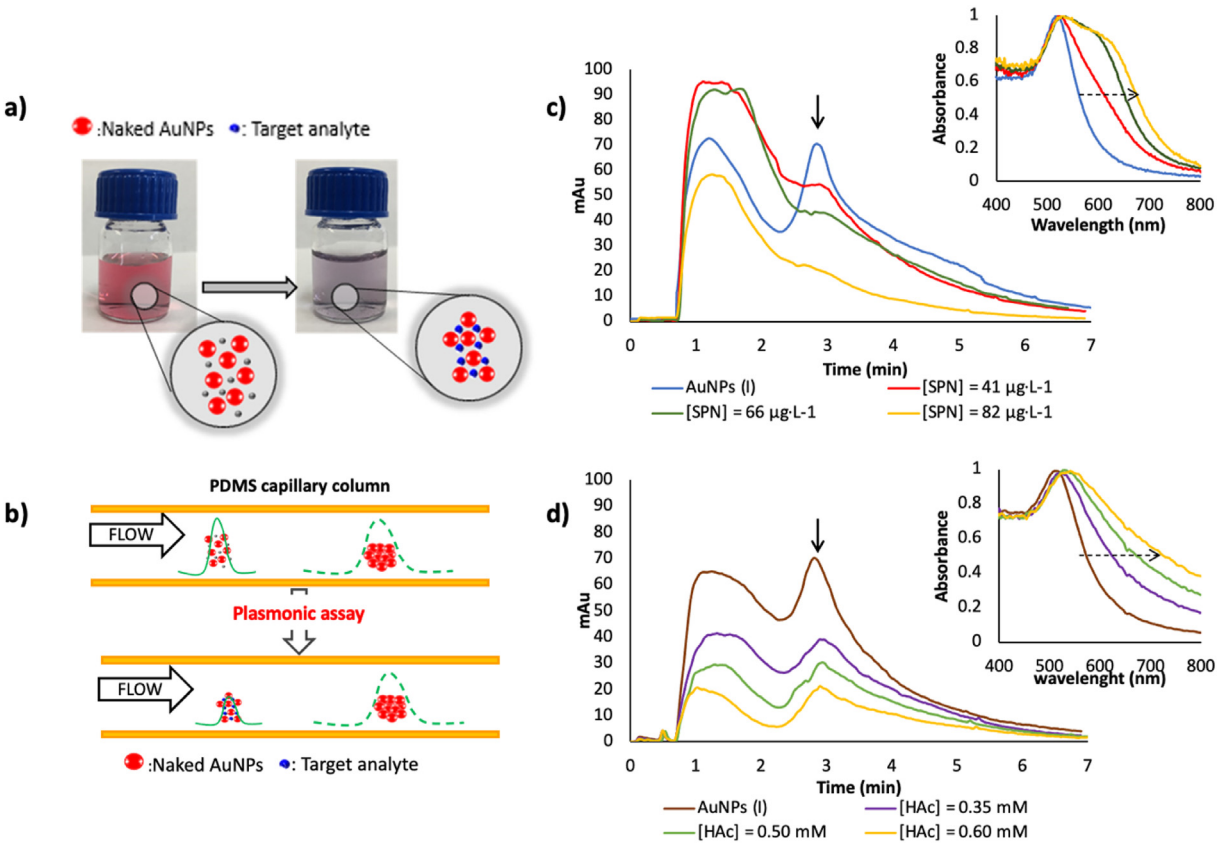

Fig. 5. (a) Schematic representation of the visual inspection, (b) Variation of the chromatographic profiles inside of the capillary column in presence of target analyte, (c) Chromatograms obtained for naked AuNPs(I) as a function of the added concentration of SPN [41 μg L^{-1} in red, 66 μg L^{-1} in green and 82 μg L^{-1} in yellow]; and (d) chromatograms obtained for AuNPs(I) as function of the added concentration of HAc [0.35 mM in purple, 0.50 mM in green and 0.60 mM in yellow]. Insets: variation of the LSPR band of the chromatographic peak at $t_r = 3.0$ min with the successive additions of target analyte. (For interpretation of the references to color in this figure legend, the reader is referred to the Web version of this article.)

inset). This aggregation was also observed in the decrease of the chromatographic peak at $t_r = 3.1$ min, which corresponded to the signal provided for non-polarized AuNPs in the bulk distribution. Moreover, it must be highlighted that it was possible to correlate the SPN concentration and the chromatographic area of this second peak. This fact can mean that non-polarized NP population is responsible of aggregation due to SPN. The linear regression equation was Area = (670 ± 54) + (−7600 ± 700)[SPN]; $R^2 = 0.99$. It should be remarked that peak area was defined and calculated integrating the first and second chromatographic peak from their respective baselines to the inflection point corresponding to the coleution of both NPs populations.

Fig. 5d shows the variation of the chromatographic profiles as a function of the added concentration of HAc (0.35, 0.50 and 0.6 mM). It was observed that under the experimental conditions, both chromatographic signals decreased as a function of the added acid and their ratio remains unchanged, and this decrease was correlated with the HAc concentration. The same study was carried out by using naked AuNPs(II). Fig. 6 shows the chromatographic profiles of AuNPs(II) as a function of different additions of SPN (a) and acetic acid (b).

Contrary to the results obtained with AuNPs(I), monitoring of the plasmonic assay evolution using AuNPs(II) for SPN was not possible since in this case (Fig. 6a for spermine), the working concentration interval was shortened, since AuNPs(II) were completely aggregated by adding low SPN concentrations (41 and 66 μg L^{-1}). Thus, these NPs were limited to be applied for this plasmonic assay since the concentration discrimination was very poor. Acidity analysis with AuNPs(II) provided aggregation upon the addition of HAc at different levels of concentration (0.35, 0.40 and 0.50 mM) (Fig. 6b). The kinetic aggregation was accelerated at pH acidic values since it helps to promote electrostatic bridging between different NPs and depends not only on the pH but also on the counterion [21,22]. To demonstrate this effect in the naked AuNPs, the influence of different acids was studied (acetic acid, phosphoric acid and hydrochloric acid) by measuring the decrease of the peak area as a function of the $[H^+]$ for each acid. The results indicated a linear correlation between peak area and $[H^+]$ concentration for the three acids (R^2 = 0.99, 0.99 and 0.999 for CH_3COOH, H_3PO_4 and HCl, respectively). However, the slopes were −8600 ± 800 mM, −1700 ± 200 mM and −556 ± 17 mM for CH_3COOH, H_3PO_4 and HCl, respectively. This suggested that, at least under the experimental conditions of this work, aggregation is produced by a decrease on the ʒ-potential and this decrease bridged of one nanoparticle to another by cross-linking inducing the aggregation. To demonstrate this, ʒ-potential of three different batches of AuNPs before and after the aggregation was measured. The values before aggregation were −37 ± 1, −36.3 ± 0.1 and −34 ± 1 mV, for the three batches analyzed. After the addition of CH_3COOH, these valued decreased to −19 ± 3, −22 ± 1 and −19 ± 1 mV, for the three batches, respectively. The counterion imparting the strongest repulsive inter-particle interaction due to a higher charge density facilitated the dispersion stability, and therefore the lowest slope. It should be noted, that this effect was only observed in acidic conditions, since the addition of the corresponding salts (CH_3COONa, Na_2HPO_4 and KCl), did not showed variation on the signal.

Commercial NPs with different capping, citrate and phosphate, were assayed by aggregation from acetic acid. As it can be seen in Fig. 7 (a and b), different plasmonic bands were obtained in function of the capping for both, IT-SPME-NanoLC-DAD and UV−Vis spectroscopy (see Fig. 3 b and e). The kinetic of the process was slower for citrate capped AuNPs than for phosphate capped AuNPs 20 nm as discussed in the previous section. Using citrate AgNPs 20 nm the sensitivity of the assay for acetic was increased markedly as Fig. 7 (c and d) shows. These figures give the chromatograms and the spectra registered at the maximum of the two peaks for AgNPs and aggregated AgNPs adding 35 mM acetic acid. The spectra are in accordance with the kinetic obtained by UV−vis spectroscopy (see Fig. 3 c). However, the sensitivity achieved by naked AuNPs was the best (see Figure S1).

An intermediate sensitivity is obtained if mixtures of AuNPs and AgNPs are used as it can be derived from Fig. 7 (e and f), being the concentration of acid acetic used 116 mM. The chromatograms were obtained at 400 and 530 nm corresponding to the plasmonic bands of AgNPs and AuNPs, respectively. From these studies it is derived that the aggregation assay can be optimized in function on the need concentration of acetic acid to test.

3.3. Analysis of urine samples to determine SPN as a cancer biomarker as a proof of concept

To evaluate the practical application of the chromatographic method to monitor plasmonic assays, urine samples of healthy volunteers and cancer patients were analyzed following the assay described in our previous study to determine spermine (SPN) by Uv−Vis spectroscopy [5]. It should be remarked that SPN has been used as cancer biomarker in urine samples in previous studies. This

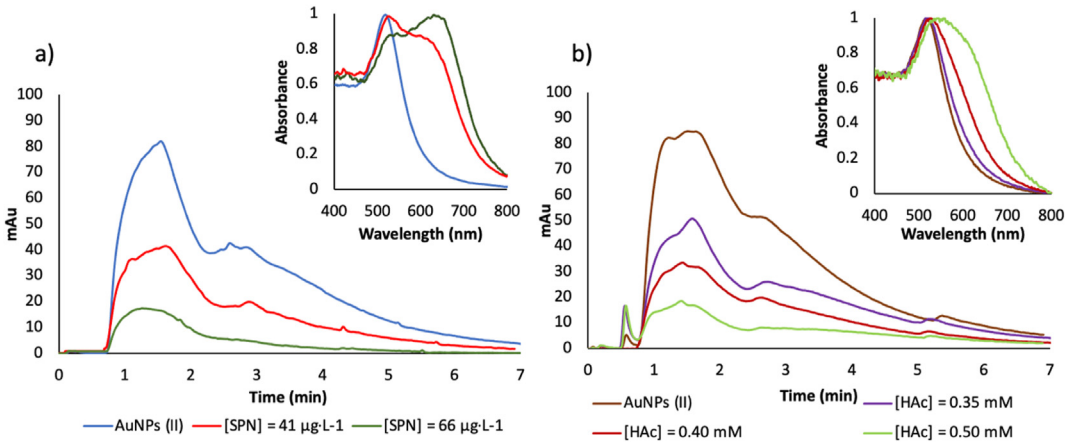

Fig. 6. Chromatograms obtained for AuNPs(II) as function of the added concentration of (a) SPN [41 μg L^{-1} in red and 66 μg L^{-1} in green] and (b) HAc [0.35 mM in purple, 0.40 mM in red and 0.50 mM in green]. Insets: variation of the LSPR band of the chromatographic peak at $t_r = 3.0$ min with the successive additions of target analyte. (For interpretation of the references to color in this figure legend, the reader is referred to the Web version of this article.)

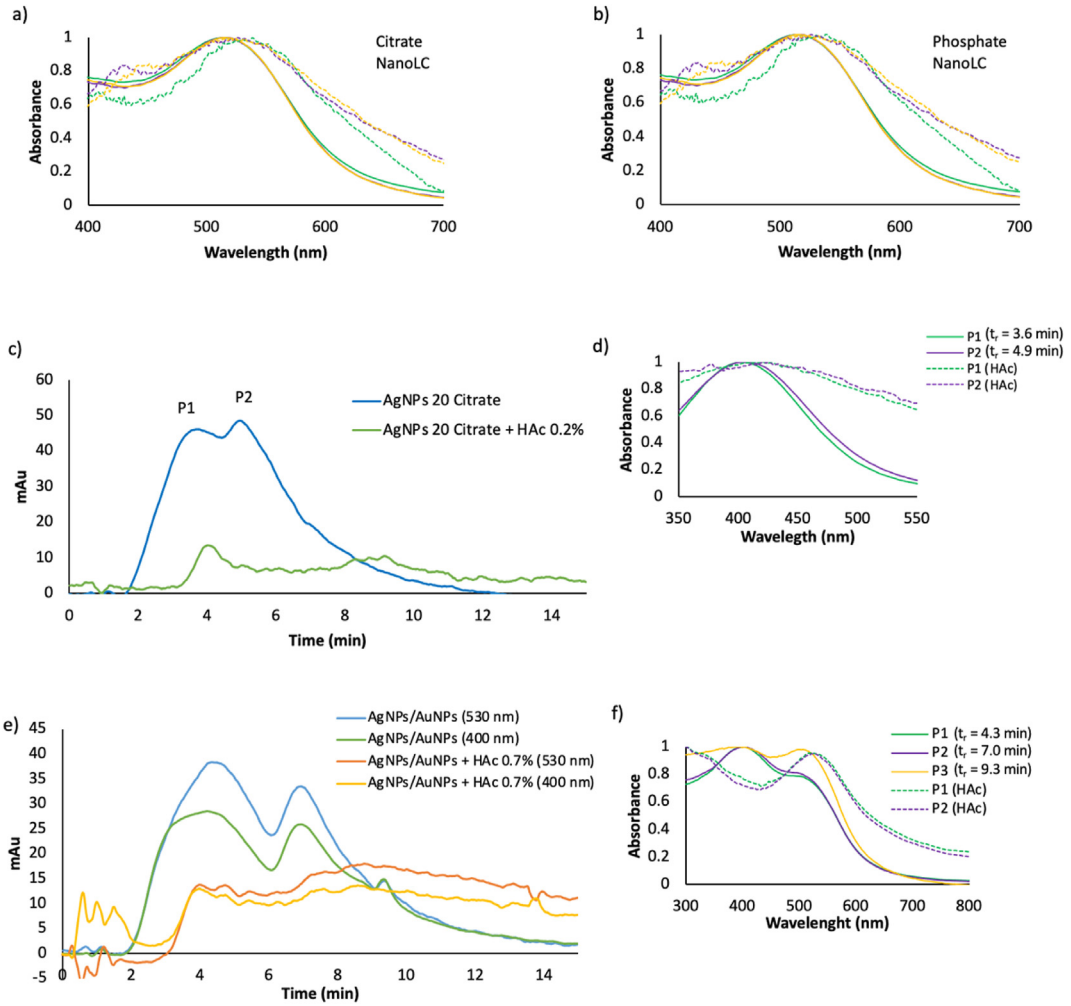

Fig. 7. Aggregation profiles of AuNPs 20 nm (a) citrate capping and (b) phosphate capping diluted 1:4 with ultrapure water by acetic acid 1.75 M; the normalized spectra were obtained at the maximum of the two chromatographic peaks (c) Chromatographic profiles of citrate capped AgNPs 20 nm diluted 1:4 with ultrapure water and their aggregation adding acetic acid 35 mM. (d) Normalized spectra at the maximum of the two chromatographic peaks of AgNPs 20 nm diluted 1:4 with ultrapure water and their aggregation by IT-SPME-nanoLC-DAD. (e) Chromatographic profiles of citrate capped AgNPs 20 nm and AuNPs 20 nm diluted 1:4 with ultrapure water and their aggregation adding acetic acid 116 mM. (f) Normalized spectra at the maximum of the three chromatographic peaks of AgNPs 20 nm and AuNPs 20 nm diluted 1:4 with ultrapure water and their aggregation by IT-SPME-nanoLC-DAD.

plasmonic assay is based on the SPN extraction by SPE with acetic acid (see Experimental section). Therefore, contribution of both compounds must be taken into account. Extracted analyte was then added to the AuNPs dispersion in order to obtain the LSR analytical signal through the chromatographic analysis. Moreover, this assay was carried out for healthy volunteers and for cancer patients in order to study the variation in the chromatographic profiles.

Fig. 8 show the chromatographic profiles when urine samples from healthy volunteer sample (Fig. 8a) and cancer patient sample (Fig. 8b) were processed. As can be seen, chromatographic profiles allowed detecting differences in the SPN content in healthy volunteers compared with cancer patients, since aggregation in the former were lower and any change in the ratio of the two chromatographic peaks was obtained. The variation of profiles was related with the SPN concentration in each type of sample which was correlated to the presence of the cancerous processes [5]. In this previous study, it was demonstrated that SPN can be used as an biomarker of cancerous processes and can be selectively detected by aggregation of naked AuNPs, after an SPE step to extract the amine.

In order to understand the differences with UV–Vis measurements, the same samples were analyzed with UV–Vis spectrophotometry (Fig. 8c and d for healthy and cancer patients, respectively). In this assay, urine for healthy volunteer and patient was added to AuNPs(I) and the spectroscopy signal was recorded for 3 min in intervals of 20 s.

As above mentioned, spectroscopic signal provided a lower sensitivity than chromatographic signal. Indeed, aggregation for healthy volunteer was not observed, even at reaction time comparable with the retention times obtained in the chromatographic system (Fig. 8a). In the case of cancer patients, the aggregation was observed as a function of the contact time when using spectroscopy, but with lower sensitivity compared with the analytical response reached with chromatography.

Finally, quantification of SPN in the cancer patient sample by using IT-SPME-CapLC-DAD was evaluated. Fig. 9 shows the chromatographic profiles for AuNPs(I), acid extract and SPN at different concentration level was added and the variation when the SPN was performed (see experimental section). As can be seen, the addition of AuNPs to a urine sample induced AuNPs aggregation, its response can be quantified and therefore, the SPN concentration in urine sample can be estimated. SPN can be estimated by taking as analytical response the difference between blank signal

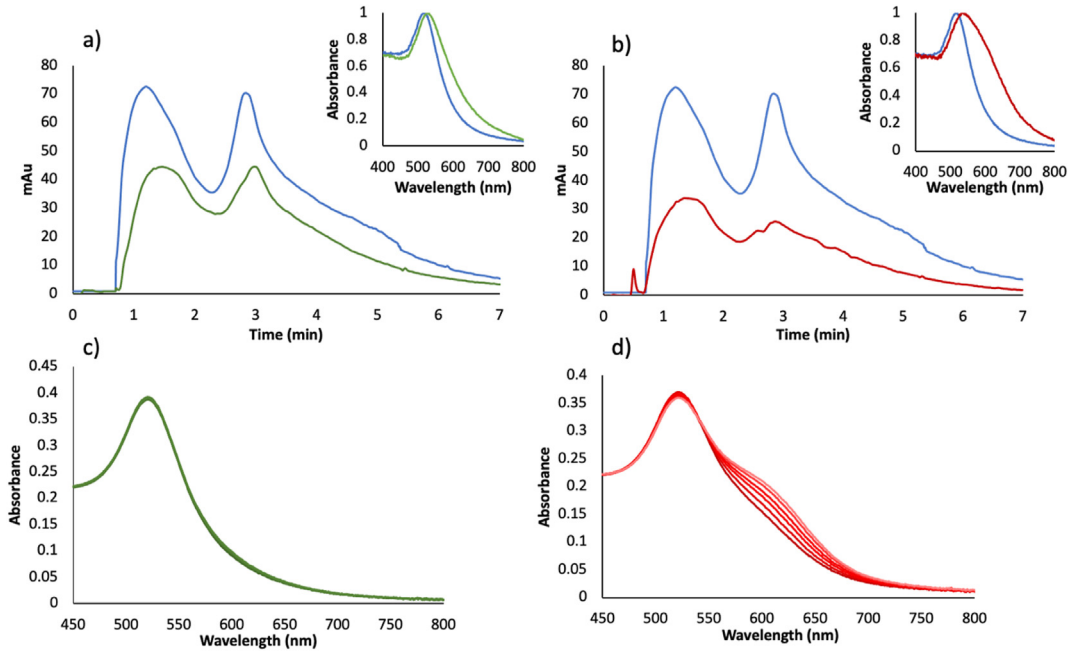

Fig. 8. Chromatographic profiles of AuNPs(I) for (a) healthy volunteer sample and (b) cancer patient sample. Insets: LSPR band variation for the chromatographic peak at $t_r = 3.0$ min. Kinetic spectroscopy study for 3 min in intervals of 20 s for (c) healthy volunteers and (d) cancer patients.

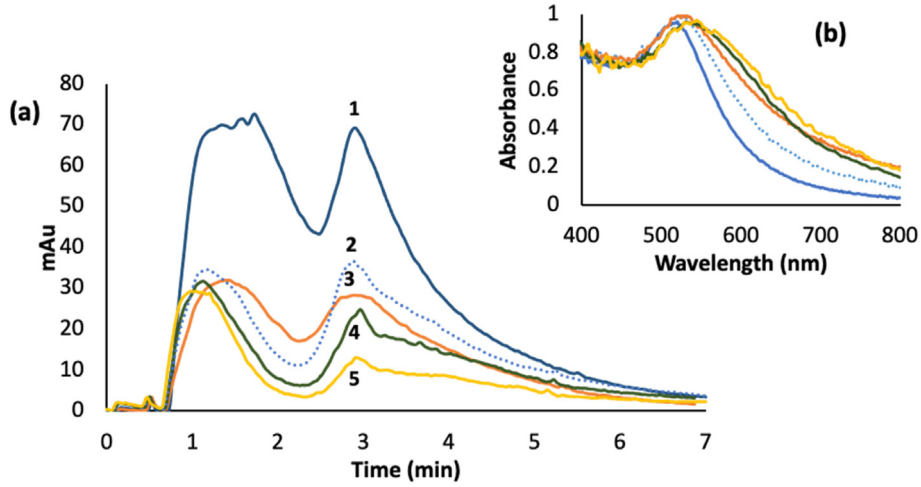

Fig. 9. (a) Chromatographic profiles obtained for 1: AuNPs(I), 2: blanc acidic extract (HAc), 3: Urine sample, 4: urine sample spiked with 16 μg L^{-1} of SPN and 5: urine sample spiked with 26 μg L^{-1} of SPN. (b) UV spectra corresponding to peak chromatogram at 3 min.

($t_r = 3.1$ min) and the signal of the SPN spikes. The results indicated a linear correlation Area= $(-3\pm8) + (8400 \pm 500)$[SPN]; $R^2 = 0.9969$. Finally, using this equation, the SPN concentration in urine can be estimated, and it was 83 μg L^{-1}. This result was in agreement with the results given in the previous work [5].

4. Conclusions

The present study demonstrates the potential of IT-SPME-MiniaturizedLC-DAD for assessment of noble metal NPs for developing reliable plasmonic assays. Besides it takes also advantage of the LSPR of naked AuNPs as analytical signal to monitor plasmonic assays. This new tool provides better sensitivity and selectivity for developing plasmonic tests than UV–Vis spectrometry. The fundamentals of the method rely on the interactions of NPs with the extractive phase immobilized inside of the IT-SPME capillary. The results indicated that these interactions gave rise to a characteristic chromatographic profile based on two chromatographic peaks, which are related with polarized and non-polarized populations in the bulk dispersion. The ratio of the two peaks conditioned their application in plasmonic assays. Commercial and naked NPs were assayed and SPN and $[H^+]$-induced assays have been tested as targets. It is demonstrated that the chromatographic profile of a given NP dispersion, carried out in less than 10 min, assures its utility in a given plasmonic assay.

To demonstrate the practical application as a proof of concept, urine samples from different cancer patients have been analyzed, since SPN has been proposed as a cancer biomarker, with successful results. Both, naked AuNPs suitability for this assay developed in Ref. [5] by UV–vis spectroscopy and the assay developing, were

carried out by the new tool proposed. Particularly, the key advantage of the employment of this separation-based method is the enhancement of the sensitivity of the previous urine assay and the potential application to isolate different phenomena that influence the LSPR signal.

CRediT authorship contribution statement

L. Sanjuan-Navarro: Investigation, Methodology, Writing – original draft. **S. Cortés-Bautista:** Investigation, Methodology. **Y. Moliner-Martínez:** Conceptualization, Investigation, Methodology. **P. Campíns-Falcó:** Conceptualization, Investigation, Methodology, Supervision, Resources.

Declaration of competing interest

The authors declare that they have no known competing financial interests or personal relationships that could have appeared to influence the work reported in this paper.

Acknowledgements

EU FEDER and the Gobierno de España MCIU-AEI (CTQ2017-90082-P) and to the Generalitat Valenciana (PROMETEO Program 2020/078) and EU FEDER- Generalitat Valenciana (ID-FEDER/2018/049). L. Sanjuan Navarro expresses his gratitude for the FPU-grant (MCIU-AEI) and S. Cortés-Bautista expresses his gratitude for the FPI-grant (MCIU-AEI).

Appendix A. Supplementary data

Supplementary data to this article can be found online at https://doi.org/10.1016/j.aca.2021.338665.

References

[1] T. Yu, Q. Wei, Plasmonic molecular assays: recent advances and applications for mobile health, Nano Research 11 (2018) 5439–5473, https://doi.org/10.1007/s12274-018-2094-9.
[2] Z. Zhang, H. Wang, Z. Chen, X. Wang, J. Choo, L. Chen, Plasmonic colorimetric sensors based on etching and growth of noble metal nanoparticles: strategies and applications, Biosens. Bioelectron. 114 (2018) 52–65, https://doi.org/10.1016/j.bios.2018.05.015.
[3] W. Zhou, X. Gao, D. Liu, X. Chen, Gold nanoparticles for in vitro diagnostics, Chem. Rev. 115 (19) (2015) 10575–10636, https://doi.org/10.1021/acs.chemrev.5b00100.
[4] D. Vilela, M.C. Gonzalez, A. Escarpa, Sensing colorimetric approaches based on gold and silver nanoparticles aggregation: chemical creativity behind the assay. A review, Anal. Chim. Acta 751 (2012) 24–43, https://doi.org/10.1016/j.aca.2012.08.043.
[5] N. Jornet Martinez, M. Gonzalez Bejar, Y. Moliner Martínez, P. Campíns Falcó, J. Pérez Prieto, Sensitive and selective plasmonic assay for spermine as biomarker in human urine, Anal. Chem. 86 (2014) 1347–1351, https://doi.org/10.1021/ac404165j.
[6] J.R. Bhamore, Z.V.P. Murthy, S.K. Kailasa, Fluorescence turn-off detection of spermine in biofluids using pepsin mediated synthesis of gold nanoclusters as a probe, J. Mol. Liq. 280 (2019) 18–24, https://doi.org/10.1016/j.molliq.2019.01.132.
[7] S.K. Kailasa, M.L. Desai, S.H. Baek, L.T. Phan, T.P. Nguyen, R. Rafique, T.J. Park, Independent spectral characteristics of functionalized silver nanoparticles for colorimetric assay of arginine and spermine in biofluids, New J. Chem. 43 (2019) 17069–17077, https://doi.org/10.1039/c9nj04132j.
[8] K.A. Rawat, J.R. Bhamore, R.K. Singhal, S.K. Kailasa, Microwave assisted synthesis of tyrosine protected gold nanoparticles for dual (colorimetric and fluorimetric) detection of spermine and spermidine in biological samples, Biosens. Bioelectron. 88 (2017) 71–77, https://doi.org/10.1016/j.bios.2016.07.069.
[9] D. Wen, W. Liu, A.K. Hermann, M. Holzschuh, F. Simon, A. Eychmüller, Simple and sensitive colorimetric detection of dopamine based on assembly of cyclodextrin-modified Au nanoparticles, Small 12 (2016) 2439–2442, https://doi.org/10.1002/smll.201503874.
[10] M.T. Alula, L. Karamchand, N.R. Hendricks, R. Nicolette, J.M. Blackburn, Citrate-caped silver nanoparticles as a probe for sensitive and selective colorimetric and spectrophotometric sensing of creatinine in human urine, Anal. Chim. Acta 1007 (2018) 40–49, https://doi.org/10.1016/j.aca.2017.12.016.
[11] Baetsen Young, A. M, M. Vascher, L.l. Matta, P. Colgan, E.C. Alocilja, B. Day, Direct colorimetric detection of unamplified pathogen DNA by dextrin capped gold nanoparticle, Biosens. Bioelectron. 101 (2018) 29–36, https://doi.org/10.1016/j.bios.2017.10.011.
[12] N. Holme, S. Rana, H.M.G. Barriga, U. Kauscher, N.J. Brooks, M.M. Stevens, A robust liposomal platform for direct colorimetric detection of Sphingomyelinase enzyme and inhibitors, ACS Nano 12 (2018) 8197–8207, https://doi.org/10.1021/acsnano.8b03308.
[13] S.K. Kailasas, J.R. Koduru, M.L. Desai, T.J. Park, R. Kumar Singhal, H. Basu, Recent progress on surface chemistry of plasmonic metal nanoparticles for colorimetric assay of drugs in pharmaceutical and biological samples, Trends Anal. Chem. 105 (2018) 106–120, https://doi.org/10.1016/j.trac.2018.05.004.
[14] V. Amendola, R. Pilot, M. Frasconi, O.M. Marago, M.A. Iata, Surface plasmon resonance in gold nanoparticles: a review, J. Phys. Condens. Matter 29 (2017) 203002, https://doi.org/10.1088/1361-648X/aa60f3.
[15] L. Sanjuan-Navarro, A. Boughbina-Portolés, Y. Moliner-Martínez, P. Campíns-Falcó, Aqueous dilution of noble NPs bulk dispersions: modeling instability due to dissolution by AF4 and stablishing considerations for plasmonic assays, Nanomaterials 10 (2020) 1802, https://doi.org/10.3390/nano10091802.
[16] R.A. Gonzalez-Fuenzalida, Y. Moliner-Martínez, C. Molins-Legua, V. Parada-Artigues, J. Verdú-Andrés, P. Campins-Falcó, New tools for characterizing metallic nanoparticles: AgNPs, a case study, Anal. Chem. 88 (2016) 1485–1493, https://doi.org/10.1021/acs.analchem.5b04751.
[17] R.A. Gonzalez-Fuenzalida, Y. Moliner-Martínez, C. Molins-Legua, P. Campíns-Falcó, Miniaturized liquid chromatography coupled on-line to in-tube solid-phase microextraction for characterization of metallic nanoparticles using plasmonic measurements. A tutorial, Anal. Chim. Acta 1045 (2019) 23–41, https://doi.org/10.1016/j.aca.2018.07.073.
[18] Y. Moliner-Martinez, A. Ballester-Caudet, J. Verdu-Andres, R. Herraez-Hernandez, C. Molins-Legua, P. Campins-Falco, In tube solid phase microextraction. Handbooks in Separation science, solid phase extraction. Ed.; Colin F. Poole, Elsevier Amsterdam (2002) 387–427, https://doi.org/10.1016/B978-0-12-816906-3.00014-5.
[19] P. Serra-Mora, N. Jornet-Martínez, Y. Moliner-Martínez, P. Campíns-Falcó, In tube-solid phase microextraction-nano liquid chromatography: application to the determination of intact and degraded polar triazines in waters and recovered struvite, J. Chromatogr. A 1513 (2017) 51–58, https://doi.org/10.1016/j.chroma.2017.07.053.
[20] G.L. Hallett-Tapley, C. D'alfonso, N.L. Pacioni, C.D. McTiernan, M. Gonzalez-Bejar, O. Lanzalunga, E.I. Alarcon, J.C. Scaiano, Gold nanoparticle catalysis of the cis–trans isomerization of azobenzene, Chem. Commun. 49 (2013) 10073, https://doi.org/10.1039/c3cc41669k.
[21] C.J. Bueno Alejo, C. D'Alfonso, N.L. Pacioni, M. Gonzalez Bejar, M. Grenier, O. Lanzalunga, E.I. Alarcon, J.C. Scaiano, Ultraclean derivatized monodisperse gold nanoparticles through laser drop ablation customization of polymorph gold nanostructures, Langmuir 28 (2012) 8183–8189, https://doi.org/10.1021/la3010689.
[22] G. Palazzo, G. Valenza, M. Dell'Aglio, A. De Giacomo, On the stability of gold nanoparticles synthesized by laser ablation in liquids, J. Colloid Interface Sci. 489 (2017) 47–56, https://doi.org/10.1016/j.jcis.2016.09.017.